# Iceshocks Observed at the Ice Sheet Surface near Mizuho Station, East Antarctica

Kenji ISHIZAWA*

# みずほ基地における氷震の観測

石 沢 賢 二*

**要旨**：みずほ基地（72°42′S, 44°20′E, 海抜 2230 m）において氷震の観測が行われた．観測は1978年5月から翌年の1月までの長期間行われた．これにより氷震のおこる条件は，気温と気温変化率との関数として表されることがわかった．そして発生の機構は雪をマックスウェル物体と仮定して説明された．

氷震の震源の決定が行われた．*P* 波の初動は観測システムのノイズにより判別できなかったので，表面波の最大振幅が用いられた．この方法の妥当性は人工的震源によって発生させた *P* 波と表面波の観測による震源計算によって確かめられた．

ある群発氷震のうちの45個の氷震について震源が決定された結果，震源はサーマルクラックのよく発達した "glazed surface" に集中した．このことにより，氷震はサーマルクラックが発生するときの震動であることが証明された．

震源の時間的移動に規則性はなく，"glazed surface" 上のあらゆるところで無規則におこることがわかった．

***Abstract*:** The seismological observation of iceshocks was carried out at Mizuho Station (72°42′ S, 44°20′ E, 2230 m a. s. l.), East Antarctica, during a period from May 1978 to January 1979. From the observation it was found that the condition of iceshock occurrence was expressed by a function of both the air temperature and the changing rate of the temperature. The iceshock occurrence was explained by the fracture of the surface snow which was assumed to be a Maxwell substance.

The focus positions of 45 iceshocks of a swarm were calculated by using the observed velocity of surface wave. This calculation was checked by the result of an artificial hitting on the snow surface and was found to be efficient for the determination of the focus position. The result of the calculation indicated that the focus positions were concentrated at the glazed surface where snow accumulation did not take place for a long time (for example, 2 or 3 years) and the fracture

* 国立極地研究所. National Institute of Polar Research, 9-10, Kaga 1-chome, Itabashi-ku, Tokyo 173.

cracks were observed. Therefore, it is concluded that the iceshocks are defined as a vibration caused by the fracture crack formation at the glazed surface due to a rapid decrease in the air temperature.

## 1. Introduction

In this paper the iceshock is defined as a vibration which occurs when ice or snow texture of ice sheet is fractured by thermal stress, and is distinguished from the shocks of tectonic origin caused by the movement of glacier or ice sheet. An iceshock is also called a thermal shock because it occurs by thermal stress owing to a rapid decrease in the air temperature.

The cracks caused by the thermal stress are developed at the glazed surface near Mizuho Station (70°42′ S, 44°22′ E, 2230 m a. s. l.), but they cannot be observed in the coastal region. The formation of the cracks seems to be a characteristic phenomenon only in the katabatic wind zone.

KAMINUMA and TAKAHASHI (1975) carried out the seismological observation of iceshock at Mizuho Station in September 1973, and found that the occurrence depended upon the air temperature and its decreasing rate. They reported that iceshocks, mostly of swarm type, occur when the air temperature is below −35°C, and the decreasing rate is −2.5°C per hour, or the lowering of about −1°C/h continues for a few hours. In their observation, complete wave trace of the shock was not obtained because they used a low frequency seismograph with 1 Hz natural frequency while the vibration frequency of the shock is much higher. Since the sound of the iceshocks was heard in an observation room at Mizuho Station, the frequency of the wave was estimated to be about 100 Hz to 1 kHz.

In order to make clear the mechanism of iceshock occurrence the seismological observations were carried out from May 1978 to January 1979 at Mizuho Station. In the present study, on the basis of the observation the focus of the iceshock was determined and the mechanism of the iceshock and the development of the crack was discussed.

## 2. Measurement

The iceshock observation system is composed of six vertical component geophones with 28 Hz natural frequency (Geo-Space Corporation, GS-30) and recording systems using a 6-ch. data recorder (TEAC Co., R-81) and a 3-ch.

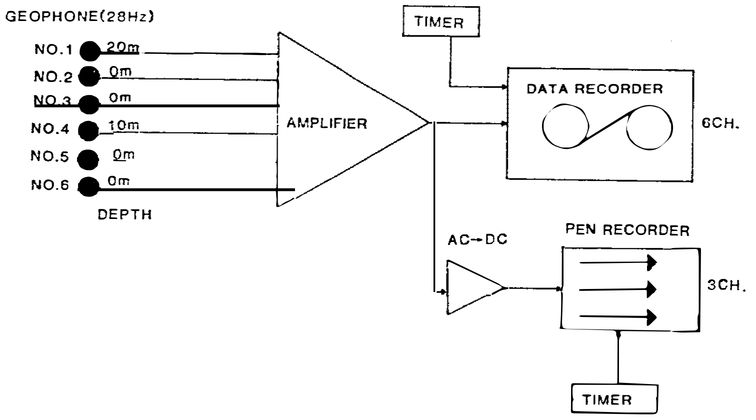


*Fig. 1. Iceshock observation system.*

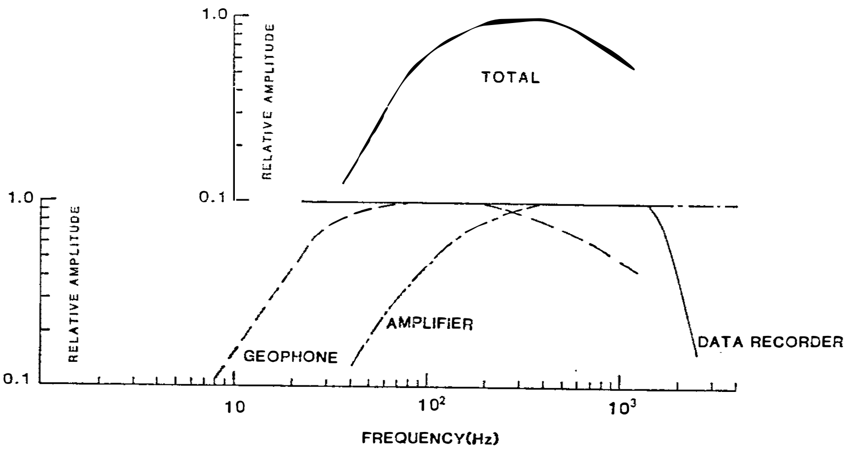


*Fig. 2. Frequency characteristics of observation system. Dashed, doted and solid curves denote those of geophone, amplifier and recorder respectively, and total characteristic of them is shown by solid line.*

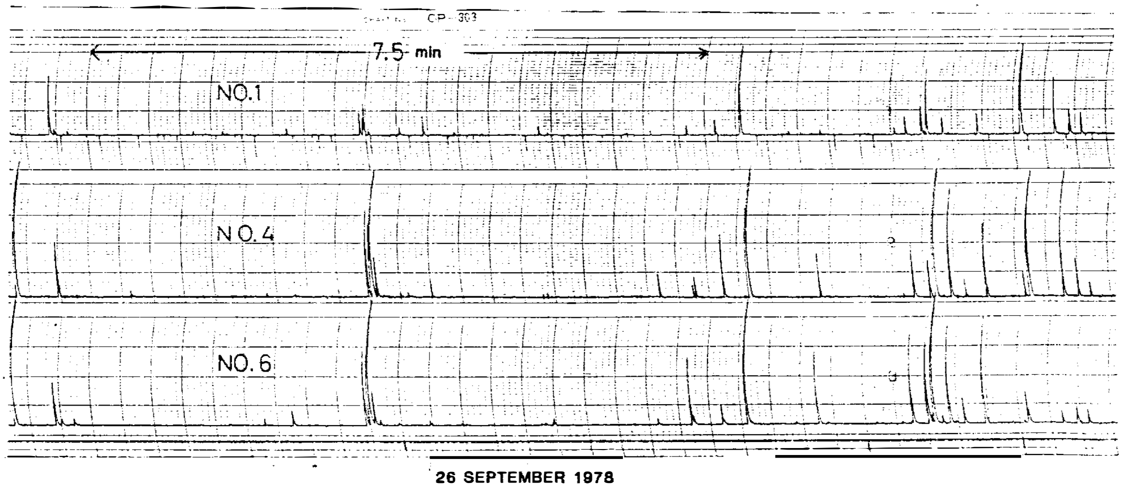


*Fig. 3. An example of records by pen-recorder during an iceshock swarm. Nos. 1, 4 and 6 denote geophones' number.*

pen-recorder (Watanabe Co., WTR-211), as shown in Fig. 1. The data recorder was used for occasional measurements of complete wave form of the iceshock. Continuous measurements were made during iceshock swarms by means of the pen-recorder in order to observe the number and the amplitude of the iceshock as a monitor. A rectifying circuit (AC → DC) was specially inserted between the amplifier and the pen-recorder for recording the average amplitude of iceshock wave because the frequency of the iceshock wave was too high to record by the pen-recorder. The frequency characteristics of geophones, amplifiers, data recorder and the total system of them are shown in Fig. 2. Four geophones were set on the snow surface and two were set at the bottom of 10 m (No. 4) and 20 m (No. 1) deep boreholes drilled with a CRREL type hand auger.

An example of the recorded iceshock of a swarm by 3-ch. pen-recorder is shown in Fig. 3. This figure shows that pulses of each trace are identified with iceshocks, and the amplitude of a pulse signifies the average amplitude of the iceshock.

Since Mizuho Station is located in the strong katabatic wind area where the mean annual wind speed is 9.9 m/s (KAWAGUCHI, 1979), drifting snow due to such katabatic wind generates the electric charge which causes a serious noise against the correct recording. During a period when the air temperature was lower than −45°C, a correct record was not obtained due to the much serious electric noise.

## 3. The Condition of the Iceshock Occurrence

KAMINUMA and TAKAHASHI (1975) carried out seismological observations of iceshock with one vertical seismograph for about half a month in September 1973 at Mizuho Station. The air temperature in September 1973 was between −20°C and −50°C. They analyzed the relations between the number of observed shocks and the air temperature, and between the number of shocks and the decreasing rate of the air temperature. They found the following conditions of the iceshock occurrence:

(1) The air temperature is below −35°C. (2) The decreasing rate of the air temperature is −2.5°C per hour or the decreasing rate is about −1°C/h but it continues for a few hours.

In order to examine the conditions, seismological measurements were

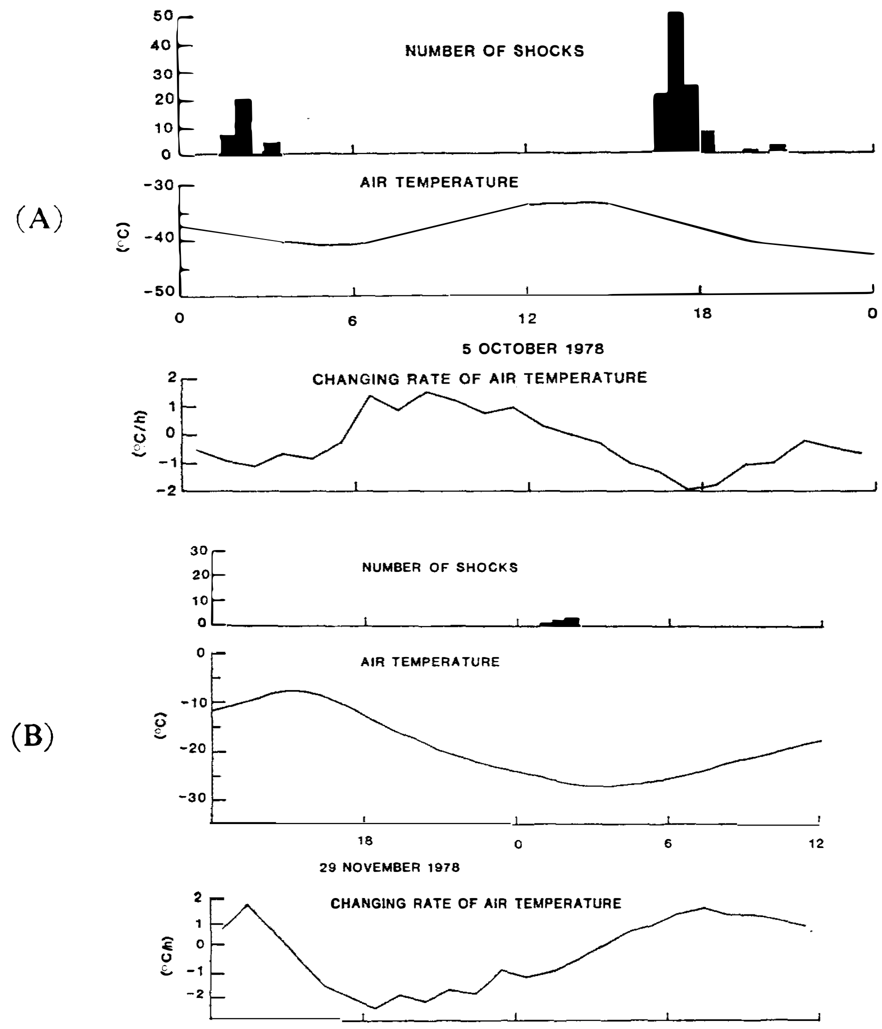


*Fig. 4. Relation between the number of iceshocks and the air temperature with the changing rate per hour. (A) A case when temperature is lower. (B) A case when temperature is higher.*

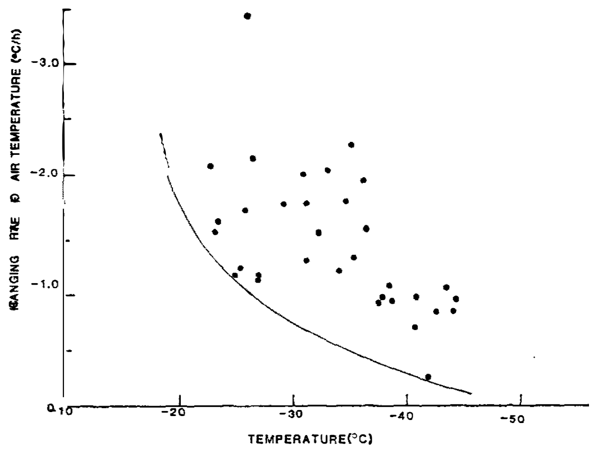


*Fig. 5. Air temperature and its decreasing rate when the first shock of iceshock swarms occur.*

carried out for a longer period from May to January. The minimum and maximum air temperatures of this period were −52.5°C on 11 and 12 August and −6.2°C on 27 December respectively. The maximum decreasing rate of the air temperature was about 4.0°C per hour. On these measurements the ralation between the iceshock occurrence and the decreasing rate of the air temperature at the time is examined. Figs. 4a and 4b show the iceshock occurrences, the air temperature and the changing rate of the air temperature.

Fig. 4 a illustrates two swarms of iceshocks observed. The first one occurred when the air temperature was −38°C and the changing rate was −1.0°C/h, the second one occurred when the air temperature was −35°C and the rate was −1.5°C/h. However, no iceshochs were observed at 18 : 00 on 29 November even though the changing rate was −2.5°C/h as shown in Fig. 4b. This suggests that the iceshock can occur under the condition of low air temperature and its rapid decrease. Fig. 5 shows the air temperature and its changing rate when the first iceshocks of the swarms occurred during the observation period. The solid line in Fig. 5 may represent critical values of the air temperature and the decreasing rate when iceshocks occur, and it indicates the conditions of the iceshock occurrence, instead of the conditions proposed by KAMINUMA and TAKAHASHI (1975).

It is intended to formulate the empirical equation of the hourly number of iceshocks in terms of air temperature $T$ and changing rate per an hour $\Delta T$ by means of multiple regression analysis. For simplification the following linear equation is assumed:

$$Y=a_0+a_1T+a_2\Delta T, \tag{3.1}$$

where $Y$ and $a_0$, $a_1$, $a_2$ are the number of iceshocks and the coefficients determined by the calculation respectively. The corelation coefficient obtained by the above calculation is 0.394; therefore, appropriate evaluation of the iceshock number cannot be achieved by the above two indices. It seems that the number of iceshocks can be explained by the temperature of shallow snow or by the temperature for a few hours before iceshocks occur.

## 4. Mechanism of Iceshock Occurrence

Many investigators including YOSHIDA (1953), KOJIMA (1954) and KINOSHITA (1957) suggested that the visco-elastic property of snow and/or ice was explained by Burgers model (Maxwell unit connected with Voigt unit in series) or Maxwell model. Therefore, in this section the mechanism of iceshock occurrence is discussed by using one-dimensional Maxwell model. The equation of Maxwell unit is as follows:

$$\frac{d\varepsilon}{dt}=\frac{1}{k}\frac{d\sigma}{dt}+\frac{\sigma}{\eta}, \tag{4.1}$$

where $\varepsilon$ is strain, $\sigma$ is normal stress, $k$ is the modulus of elasticity in tension and compression, $\eta$ is the coefficient of snow viscosity, and $t$ is time. Solving eq. (4.1) for $\sigma$ on the assumption that $d\varepsilon/dt$ is constant,

$$\sigma=k\tau\frac{d\varepsilon}{dt}(1-e^{-\frac{t}{\tau}}), \tag{4.2}$$

where $\tau\equiv\eta/k$.

Fig. 6 shows the relation between $\sigma$ and $t$ for a given strain rate, $d\varepsilon/dt=\dot{\varepsilon}$. In this figure it can be seen that the stress $\sigma$ increases gradually with time. For $t\rightarrow\infty$ eq. (4.2) is rewritten as

$$\sigma=k\tau\dot{\varepsilon}. \tag{4.3}$$

If we assume that the critical stress $\sigma^*$ is the same as a fracture stress of snow (KINOSHITA, 1957), the condition of snow fracture is expressed by

$$\dot{\varepsilon}\geqq\frac{\sigma^*}{\eta}. \tag{4.4}$$

The strain caused by a thermal stress is given by the following equation:

$$\varepsilon=\alpha\Delta T, \tag{4.5}$$

where $\alpha$ is a coefficient of thermal expansion and compression and $\Delta T$ is temperature change. Substituting $\dot{\varepsilon}=\alpha\, dT/dt$ into eq. (4.4), we can obtain the following equation as the condition of snow fracture:

$$\alpha\eta\left(\frac{dT}{dt}\right)\geqq\sigma^*. \tag{4.6}$$

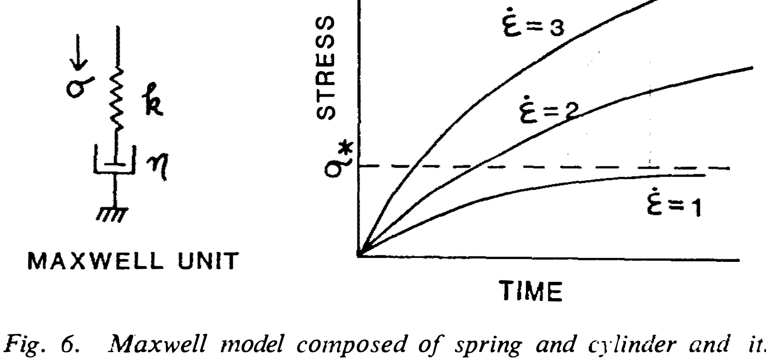


*Fig. 6. Maxwell model composed of spring and cylinder and its stress-time curves under the constant strain rates.*

YAMAJI (1957) measured the coefficient, $\alpha$, and obtained the following relation:

$$\alpha = a + bT \qquad a = 5.4\times10^{-5}\ 1/^\circ\mathrm{C},\ b = 1.8\times10^{-7}, \tag{4.7}$$

where $T$ is snow temperature in Centigrade. SHINOJIMA (1962) also carried out one-axis loading tests of snow samples and obtained an empirical equation of the viscosity coefficient in tension, $\eta$, expressed by a function of temperature and density as follows:

$$\eta = \eta_0 \exp(-0.089T), \qquad \eta_0 = 961.2 \exp(25.3\rho), \tag{4.8}$$

where $\eta_0$ is $\eta$ at 0°C, and $\rho$ is the snow density (g/cm$^3$). Multiplying eqs. (4.7) and (4.8), we obtain

$$\alpha\eta \doteqdot a\eta_0 \exp(-0.089T). \tag{4.9}$$

From eqs. (4.6) and (4.9), the condition of the first shock occurrence of a swarm is given by

$$a\eta_0 \exp(-0.089T)\frac{dT}{dt} = \sigma^*. \tag{4.10}$$

Fig. 7 indicates the relation between the rate of temperature change (°C/h) and the snow temperature for given values of $\sigma^*/a\eta_0$. The observed relation obtained in the present study is shown by a dashed line, which is similar to the curve of $\sigma^*/a\eta_0 = 10$. $\eta_0$ can be calculated for a given snow density by using eq. (4.8). The tensile strength $\sigma_T$ of dry snow is expressed by the following equation (BALLARD and FELDT, 1966; KEELER and WEEKS, 1968):

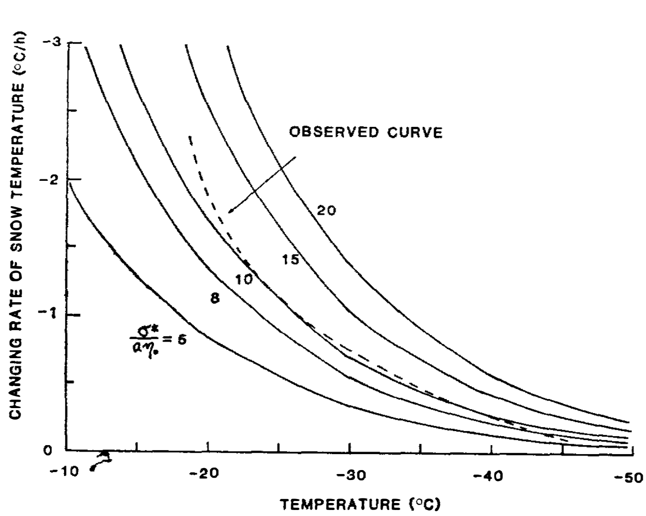


*Fig. 7. Critical curves (solid lines) of iceshock occurrence calculated theoretically and the observed one (dashed line) from Fig. 5.*

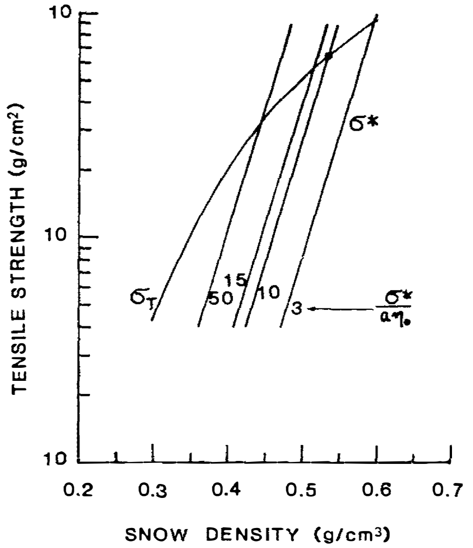


*Fig. 8. The relation between tensile strength $\sigma_T$ of snow and snow density. Destructive strength $\sigma^*$ on several $\sigma^*/a\eta_0$ is also shown.*

$$\sigma_T = 27.3 \exp\left(\frac{-2n}{1-n}\right) \qquad \text{kg/cm}^2 \qquad (4.11)$$

where $n = 1 - \rho/\rho_i$ and $\rho_i$ is the density of ice. Fig. 8 gives the relation between the tensile strength $\sigma_T$ and the desity of snow calculated with eq. (4.11). In the same figure, the fracture stress $\sigma^*$ is calculated for a given value of $\sigma^*/a\eta_0$. Fig. 8 shows that the density at a point of intersection of $\sigma_T$ and $\sigma^*$ for $\sigma^*/a\eta_0 = 10$ which explained the observed relation between $T$ and $dT/dt$ is about 0.53 g/cm$^3$, and the tensile strength (fracture stress) is about 6.4 kg/cm$^2$. $\rho = 0.53$ g/cm$^3$ is the value between the density of the glazed surface ($\rho = 0.69$ g/cm$^3$ by FUJII, 1978) and the depth hoar under the surface ($\rho = 0.4$ by WATANABE, 1977). This suggests that the cracks which cause the iceshock are formed by fractures of the glazed surface and the depth hoar layer under the surface.

## 5. Focus Determination of Iceshock

An iceshock is the vibration in snow caused by the generation of a crack. Such cracks are called "thermal cracks" because they are formed by the thermal stress (YAMADA, 1975). In the vicinity of Mizuho Station, the thermal cracks are found at the glazed surface of 2-4 mm thick multi-layered ice crust, on which no snow is deposited for a period of half a year to a few years due to strong katabatic wind (FUJII, 1979). The plane view and the vertical section of the thermal cracks are shown in Fig. 9. The width of the crack is about 3 mm to 1 cm and its depth is less than 30 cm.

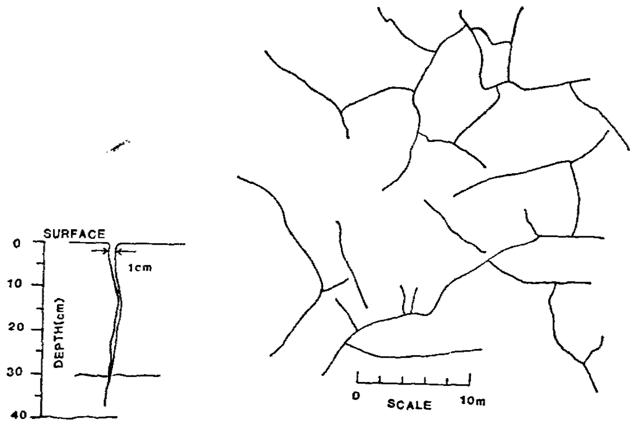


*Fig. 9. Horizontal pattern of thermal cracks and the vertical section.*

To measure the focuses of the iceshocks 6 geophones were installed about 100 m apart from each other at Mizuho Station, and the *P* wave velocity profile at Mizuho Station was obtained by the logging and the refraction method (ISHIZAWA, 1981). Though the focus of iceshock is determined by the method using the first arrival times of *P* wave obtained at several observational points, the correct recording was unsuccessful due to the trouble of the recording system. Therefore, the focuses are determined by the analysis of surface wave as is described below.

### 5.1. The method of focus determination using surface wave

ISHIZAWA (1981) carried out the measurement of the *P* wave velocity down to a depth of 36.4 m with the refraction method at Mizuho Station. The example of the measurement is shown in Fig. 10. In this figure black solid circles indicate highest amplitudes in each trace. The surface wave is

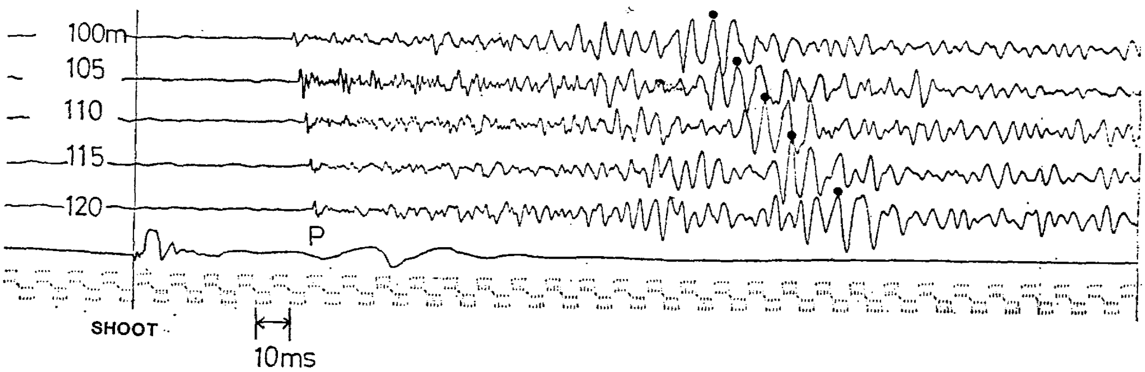


*Fig. 10. The surface waves obtained by the refraction method. Black circles indicate the maximum amplitudes of traces. P denotes the first arrivals of P wave.*

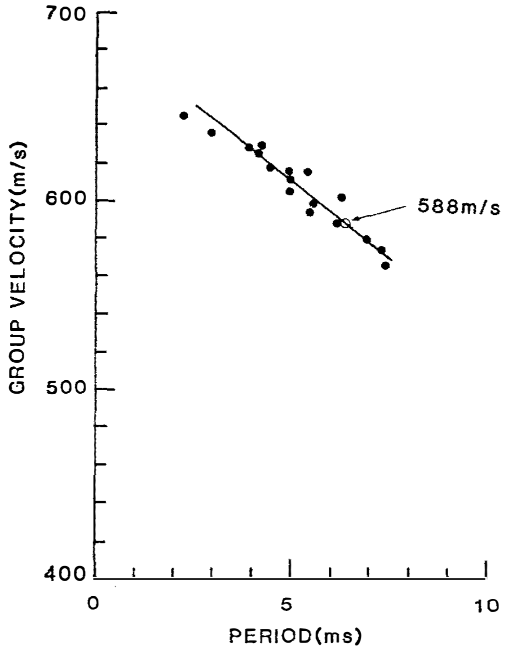


Fig. 11. *Dispersion curve of group velocity by the refraction method.*

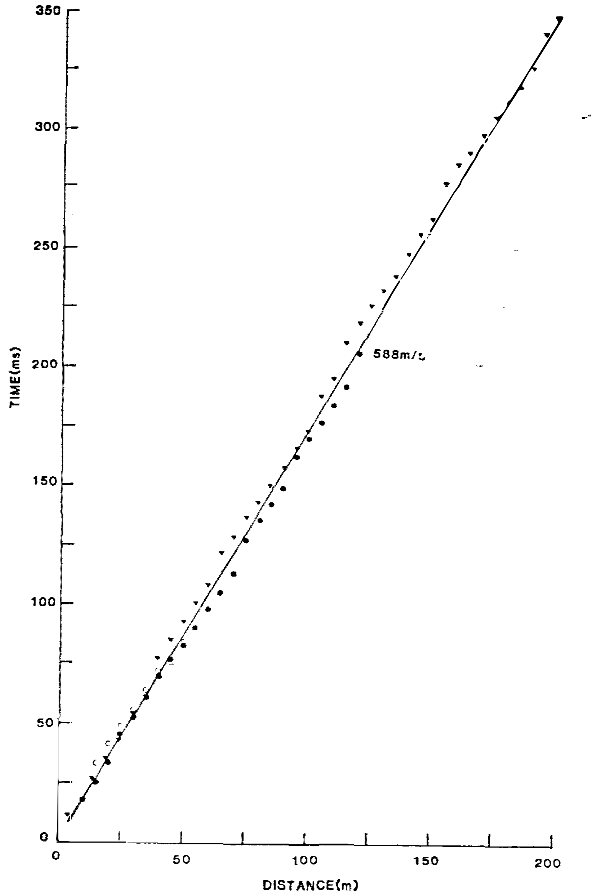


Fig. 12. *Time-distance relation of maximum amplitude of surface wave by the refraction method carried out at the three different sites (black and white circles and triangles).*

characterized by a reverse dispersion, that is, the propagating velocity of high frequency wave is faster than that of low frequency wave in each trace. The group velocity calculated from the records is shown in Fig. 11. A solid line in the figure indicates a linear relation between the group velocity and the period. The reverse dispersion seems to be caused by the high density ice at the glazed surface. Fig. 12 shows that the relation between the travel time of the maximum amplitude of the wave and the distance from a source is given by a straight line, and the velocity of the maximum amplitude is 588 m/s within the distance of 200 m. The refraction field surveys were carried out on the three different spans spread on the glazed surface, and the values obtained in these surveys are shown by black and white circles and black triangles.

The focus of iceshock is assumed to be located at the surface because the maximum depth of thermal cracks is less than 30 cm and the air temperature change resulting in iceshock is most steep at the snow surface. Therefore, the focus of iceshock should be determined by using the travel time of the maximum amplitude of surface wave. The detailed method of focus calculation is described in Appendix.

Before the method mentioned above is adopted to determine the focus of natural iceshock, the accuracy of the method was checked by the shocks generated artificially on the snow surface. The shocks were made by hitting the snow surface vertically with a wooden hammer, and the generated wave

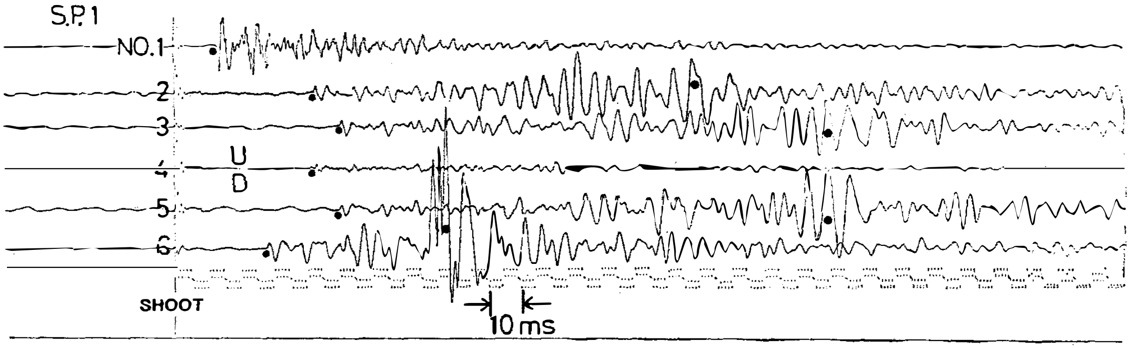


*Fig. 13. An example of observed surface wave by means of an artificial source. Large black circles denote maximum amplitudes of traces and small ones are first arrivals of P wave.*

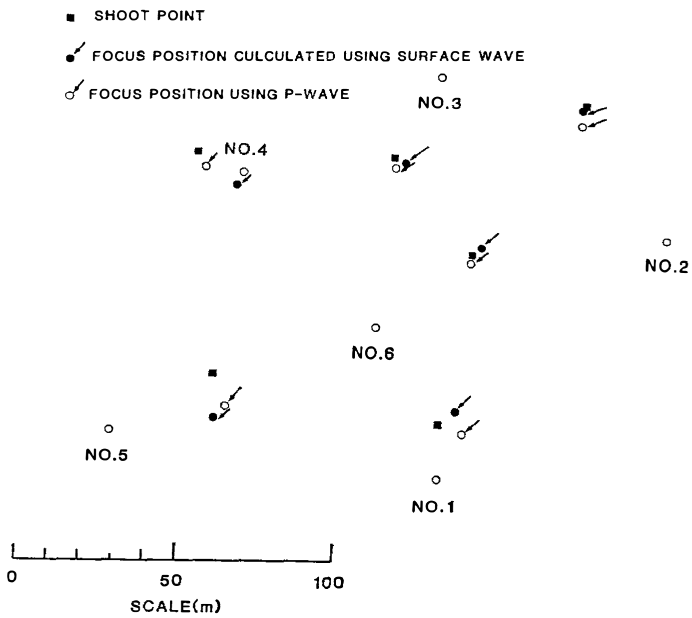


*Fig. 14. Focus positions calculated by surface wave and by P wave measurement and the true focus positions.*

was detected by the same geophones as those used in the iceshock observation shown by No. 1–No. 6 in Fig. 14. One of the records is shown in Fig. 13, in which four traces (Nos. 2, 3, 5, 6) are used for the focus determination. In the hitting method the analysis of the first arrivals of *P* wave is also used and six traces (Nos. 1–6) are examined. Small and large black circles in these traces show the first arrivals of *P* wave and the maximum amplitudes of the surface wave, respectively. The shoot points and the focus position determined by the two different methods are shown in Fig. 14. The good result of the focus determination as shown in Fig. 14 indicates that the method using the surface wave is useful to determine the focus position and the accuracy is within 10 m.

### 5.2. Position of iceshock focus

The focuses of iceshocks were determined by the method using the surface wave on 45 cases observed for two hours on 30 September 1978. These iceshocks determined are a part of the swarm which continued for about eleven hours as shown in Fig. 15. The 45 iceshocks detected by four geophones (Nos. 2, 3, 5, 6) were picked up for the calculation among the iceshocks that occurred during the hatched time on abscissa in Fig. 15. An example of the

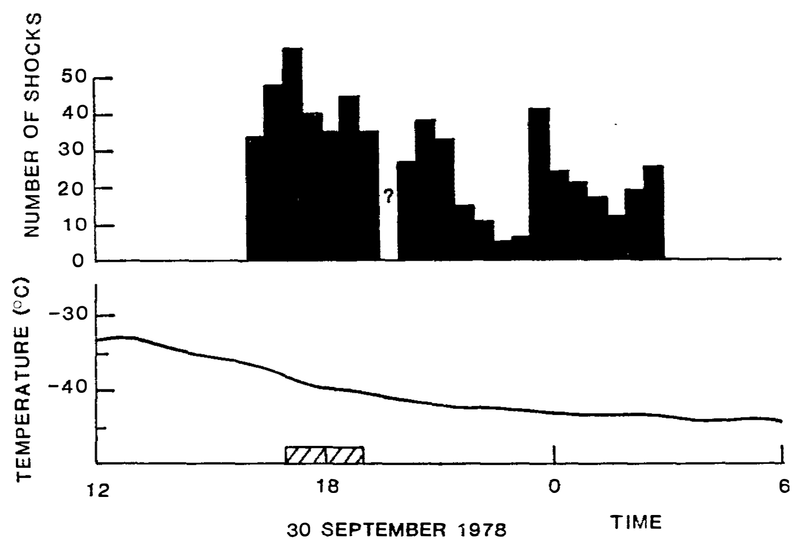


*Fig. 15. The number of iceshocks and the air temperature during the iceshock swarm on 30 September 1978 in which focus determination was carried out. The focuses of shocks for about two hours (hatched area) were determined. ? denotes unmeasured time in which radio communication noise disturbed iceshock recording.*

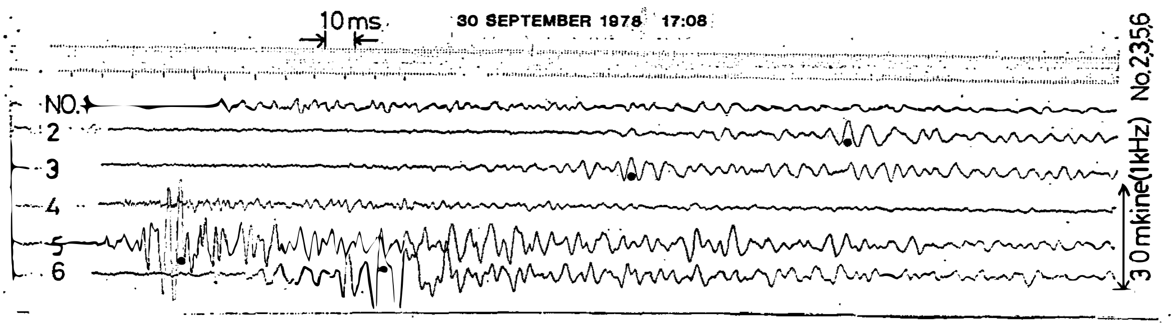


*Fig. 16. Waveform and the maximum amplitudes of a natural iceshock (black circles).*

records of the iceshocks that occurred at 17:08 on 30 September 1978 is shown in Fig. 16. The first arrivals of *P* wave on each trace cannot be identified, but the maximum amplitudes of four traces (black circles) are detected clearly. The scale of amplitudes at 1 kHz in four traces of Nos. 2, 3, 5, 6 is shown at the right end in the figure.

The calculated positions of the focuses are shown by black circles in Fig. 17. The glazed surface is shown by the hatched area where thermal cracks developed. It is clear that the calculated positions are concentrated on the glazed surface. Therefore, it is concluded that iceshock occurs as a result of thermal crack formation at the glazed surface. Fig. 18 shows the order of

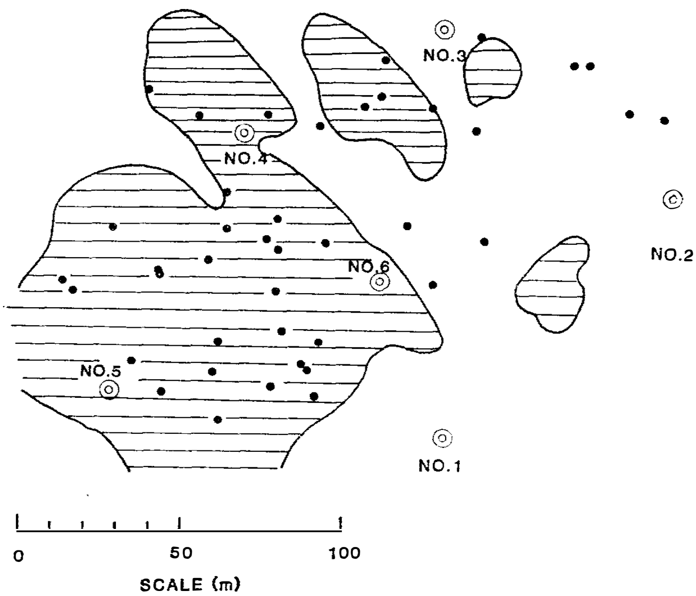


*Fig. 17. Distribution of focuses (black circles) and the observed glazed surface area. White circles, Nos. 1-6, are geophones.*

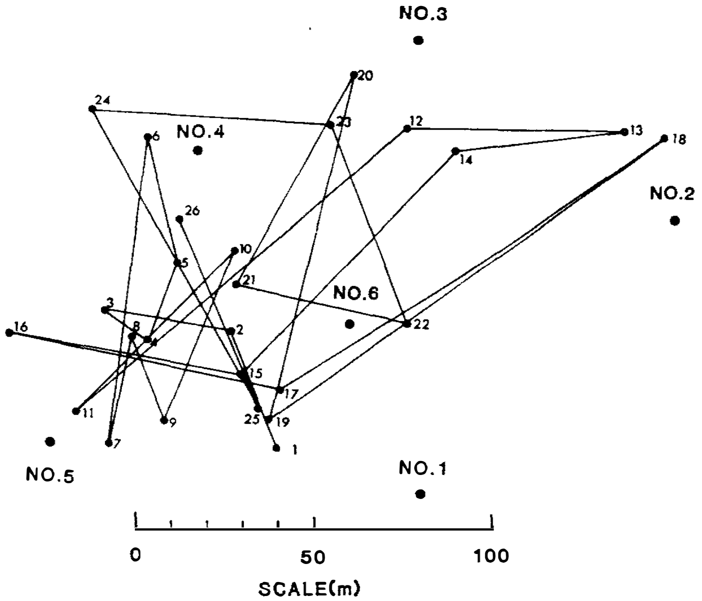


*Fig. 18. Time sequence of focuses migration. The numbers 1–25 mean the occurring order, and large black circles are geophones.*

iceshock occurrence of 26 events among 45 iceshocks determined in Fig. 17. This figure shows that iceshocks occur at random in time and position.

## Acknowledgments

I would like to express my gratitude to all members of the 19th Japanese Antarctic Research Expedition led by Prof. T. HIRASAWA for their kind encouragements and supports for the observation, especially Messrs. K. SUZUKI, K. USHIKI, S. TSUZURAHARA, S. KANETO, S. NAKAYAMA and M. EBISAWA. Also I wish to thank Drs. C. KITSUNEZAKI and K. NORITOMI of Akita University and Mr. F. NISHIO of the National Institute of Polar Research for their useful suggestions in the observation and the analysis. My thanks are also extented to Drs. S. MAE and Y. FUJII of the National Institute of Polar Research for their helpful comments on the manuscript.

## References

BALLARD, G. E. H. and FELDT, E. D. (1966): A theoretical consideration of the strength of snow. J. Glaciol., 6 (42), 159–170.

FUJII, Y. (1979): Sublimation and condensation at the ice sheet surface of Mizuho Station, Antarctica. Nankyoku Shiryô (Antarct. Rec.), 67, 51–63.

ISHIZAWA, K. (1981): The measurement of the velocities of *P* and *S* wave propagating in the surface layer of ice sheet at Mizuho Station, East Antarctica. Nankyoku Shiryô (Antarcti. Rec.), **73**, 147–160.

KAMINUMA, K. and TAKAHASHI, M. (1975): Iceshock swarms observed at Mizuho Camp, Antarctica. Nankyoku Shiryô (Antarct. Rec.), **54**, 75–83.

KAWAGUCHI, S. (1979): Meteorological data at Mizuho Station, Antarctica in 1978. JARE Data Rep., **52** (Meteorol. 6), 91 p.

KEELER, C. M. and WEEKS, W. F. (1968): Investigations into the mechanical properties of Alpine snow-packs. J. Glaciol., **7** (50), 253–271.

KINOSHITA, S. (1957): Sekisetsu ni okeru henkeisokudo to futatsuno henkei keishiki (sosei henkei, hakai henkei) to no kankei (The relation between the deformation velocity of snow and two types of its deformation. Plastic and destructive.), Teion Kagaku, Butsuri-hen (Low Temp. Sci., Ser. A), **16**, 139–166.

KOJIMA, K. (1954); Sekisetsu no nendansei (Visco-elastic property of snow), Teion Kagaku, Butsuri-hen (Low Temp. Sci., Ser. A), **12**, 1–13.

SHINOJIMA, K. (1962): Yuki-no nendanseiteki toriatsukai. Tekken Hôkoku, **328**.

YAMADA, T. (1975): Thermal cracks in snow cover at Mizuho Camp in 1971. JARE Data Rep, **27** (Glaciol.), 177.

YAMAJI, K., (1957): 0°C–100°C no hani no kôri no netsubôchô (Thermal expansion of ice in the temperature range 0°C–100°C), Teion Kagaku, Butsuri-hen (Low Temp. Sci., Ser. A), **16**, 73–77.

YOSHIDA, Z. (1953): Yuki no nendansei oyobi yuki no hakai teikô (Visco-elastic property and break-down resistance of snow), Teion Kagaku, Butsuri-hen (Low Temp. Sci., Ser. A), **10**, 1–11.

WATANABE, O. (1977); Stratigraphic observations of surface snow cover. JARE Data Rep., **36** (Glaciol.), 61–125.

*(Received April 13, 1981)*

# Appendix

## Method of focus determination

The following discussion is done on an assumption that the focuses are located at the surface. The notation in calculation is as follows:

$(x_i, y_i)$: coordinate of an observation point.

$(x, y)$ : coordinate of a focus.

$t_i$ : arrival time at an observation point.

$t$ : occurrence time of an iceshock.

$X=\{(x-x_i)^2+(y-y_i)^2\}^{\frac{1}{2}}$: distance between a focus and an observation point.

The time-distance relation of maximum amplitude of surface wave is

$$t_i-t=aX+b, \tag{A. 1}$$

where $a$ and $b$ are constants. An arrival time at an observation point is as follows:

$$t_i=a\{(x-x_i)^2+(y-y_i)^2\}^{\frac{1}{2}}+b+t. \tag{A. 2}$$

The number of the observation points located at the snow surface are four, and unknown values are three $(x, y, t)$. Therefore, we should obtain $x$, $y$ and $t$ by a non-linear least squares method. An arrival time of eq. (A. 2) is modified as follows:

$$t_i=f(x_0, y_0, t_0)+\left(\frac{\partial f}{\partial x}\right)_0\delta x+\left(\frac{\partial f}{\partial y}\right)_0\delta y+\left(\frac{\partial f}{\partial t}\right)_0\delta t, \quad (\text{A. }3)$$

where $t_i=f(x, y, t; x_i, y_i, a, b)$ (A. 4)

$$\left(\frac{\partial f}{\partial x}\right)_0=a(x_0-x_i)\{(x_0-x_i)^2+(y_0-y_i)^2\}^{-\frac{1}{2}},$$

$$\left(\frac{\partial f}{\partial y}\right)_0=a(y_0-y_i)\{(x_0-x_i)^2+(y_0-y_i)^2\}^{-\frac{1}{2}}, \quad (\text{A. }5)$$

$$\left(\frac{\partial f}{\partial t}\right)_0=1.$$

We can calculate unknown values $\delta x$, $\delta y$, $\delta t$ when $\varepsilon$ in the following equation is minimum.

$$\varepsilon=\sum_{i=1}^{n}(t_i'-t_i)^2$$

$$=\sum_{i=1}^{n}\left\{t_i'-f(x_0, y_0, t_0)-\left(\frac{\partial f}{\partial x}\right)_0\delta x-\left(\frac{\partial f}{\partial y}\right)_0\delta y-\left(\frac{\partial f}{\partial t}\right)_0\delta t\right\}^2, \quad (\text{A. }6)$$

where $t_i'$ is an observed arrival time and $n$ is the number of observation points. The normal equation of eq. (A. 6) is as follows:

$$\begin{bmatrix}[AA][AB][AC]\\ [BA][BB][BC]\\ [CA][CB][CC]\end{bmatrix}\begin{bmatrix}\delta x\\ \delta y\\ \delta t\end{bmatrix}=\begin{bmatrix}[AE]\\ [BE]\\ [CE]\end{bmatrix} \quad (\text{A. }7)$$

where $[\ \ ]=\sum_{i=1}^{n}$, $A=\left(\frac{\partial f}{\partial x}\right)_0$, $B=\left(\frac{\partial f}{\partial y}\right)_0$, $C=\left(\frac{\partial f}{\partial t}\right)_0$, $E=t_i'-f(x_0, y_0, t_0)$.

As the solution of the matrix eq. (A. 7) we can obtain $\delta x$, $\delta y$, $\delta t$. $x_0+\delta x$, $v_0+\delta y$ and $t_0+\delta t$ obtained in the step are regarded as $x$, $y$, $t$ in the next step. The same calculation is repeated untill $\delta x$, $\delta y$, $\delta t$ become sufficiently small.